The Saint Pierre Bois quarry, an analog site of the Permo-Triassic cover / Hercynian basement transition in the Rhine graben

C.LEROUGE[1], C. DEZAYES[1], A. KUSHNIR[2], C. DUEE[1], G. WILLE[1]

[1]BRGM, [2]EOST

c.lerouge@brgm.fr

Keywords: fracture network, paleo-circulations, fracture porosity

ABSTRACT

Within the frame of the ANR-funded CANTARE-Alsace project, we carried out a multi-disciplinary approach to have a better understanding of the reservoir quality at the transition zone between the sedimentary cover and the basement for the assessment of its geothermal potential. In this paper, we present the first results of a study performed on an exhumed transition zone in the quarry of Saint Pierre Bois in the Vosges Mountains, on the western flank of the Rhine graben. In this analogue of a deeply buried transition zone of the Rhine Graben, a thin layer of Stephanian-Permian sandstones is still present on the top of the fractured and altered granitic basement providing the opportunity to study in-situ the reservoir quality in this transition zone. In that aim, we focused in this paper on the fracture network, fracture fillings and petrophysical properties of the sandstones and the granite at the transition zone, as they are parameters informative of the reservoir quality during the exploration phase of a geothermal project.

1. INTRODUCTION

The formation of the Rhine Graben — which straddles the border of France and Germany — is a direct consequence of Tertiary continental rifting. This rifting created several thermal anomalies that remain of sufficiently high temperature to be economically exploitable as geothermal resources. Currently, geothermal resources are being exploited throughout the Rhine Graben including at Soultz-sous-Forêts, France (Hercynian crystalline basement at 5 km) and Rittershoffen, France (Permo-Triassic sedimentary cover/Hercynian granitic basement transition at 3 km). located on the western shoulder of the Rhine graben The overlying Tertiary sediments of the Rhine Graben act as low-permeability caprocks. Critically, thermal anomalies remain spatially restricted in the Rhine Graben and their quality varies significantly throughout the region. This regional heterogeneity in thermal anomaly quality may be related to the spatial variability of the topology of the transition zone between the Hercynian basement and overlying Mesozoic sediments.

The aim of this work is at better understanding the heterogeneities of the reservoir quality at the cover/basement transition in the Rhine graben.

For that we selected the Saint Pierre Bois quarry, located on the western shoulder of the Rhine graben, as a good analog candidate of the Permian-Triassic cover / Hercynian basement transition found at geothermally relevant depths such as Rittershoffen. In the quarry, three benches created from granulate exploitation provide a 3D picture of the subsurface. There, up to 15 meters of arkoses overly a two mica coarse-grained leucogranite.

The work approach consist into three parts. Firstly, we study the quality of the fractured reservoir in the crystalline basement by having a good knowledge of the fracture network, of the fracture cements and of the consequences of fluid/rock interaction on the matrix porosity. For that, we measured fractures and fault orientations, and observed microstructures of the different fracture type using optical and electron miscroscopy, completed by cathodoluminescence. Our sampling focussed on the porosity heterogeneities at the scale of fault structure. Secondly, we studied the quality of sandstone using optical and electron microscopy. Thirdly, we looked at the role of the paleo-weathering, and of tectonics on the topology and the porosity of the materials at the cover/basement interface. Here are presented the data only concerning samples from the back front of the quarry in which paleo-weathering is the least intense. The results of the third part are not presented.

2. SAINT PIERRE BOIS QUARRY AS AN ANALOGUE SITE

The Saint Pierre Bois quarry, 76 km south of Soultz-sous-Forêts and currently exploited for granulates, is located on the north-western border of the Dambach-Scherwiller granite (figure 1). The granite of the Saint Pierre Bois quarry is a two mica coarse-grained leucogranite crosscut by a network of aplites and pegmatites. The fresh granite samples consist of quartz (37 - 42 wt.%), K-feldspar (25 - 31 wt.%), plagioclase (25 - 29 wt.%), biotite (3 wt.%) and muscovite (3 - 4 wt.%). K-feldspar is deformed and exhibit albite exsolutions.. A layer of arkosic sediments whose thickness does not exceed 15 meters overlies the granite. Texture of detrital sediments highly depends of the morphology of the surface of the eroded granitic basement. On the back front of the quarry, products of in-situ granite dismantling filled the negative relief of the granite erosion surface (figure 2).

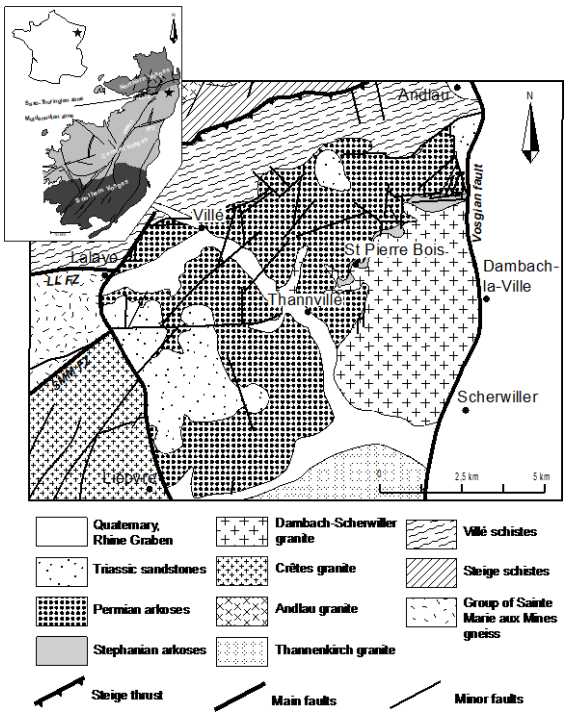

Figure 1: Geological map of the Saint Pierre Bois quarry area (from Blanalt et al., 1970)

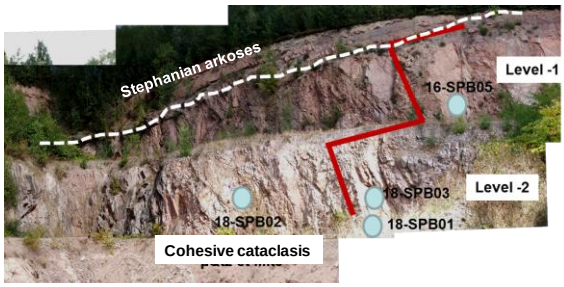

Figure 2: Back front of the Saint Pierre Bois quarry

3. RESERVOIR QUALITY OF GRANITIC BASEMENT

3.1 Orientation measurements

The granite of Saint Pierre Bois is highly fractured. More than 200 measures carried out along accessible walls of the quarry provide evidence of two major fracture sets. The main fracture set is oriented E-W and the second one NNE-SSW (Figure 3). On the backside of the quarry, the regular and highly developed network of E-W large-scale faults affecting the granite generally terminate at the sedimentary cover.

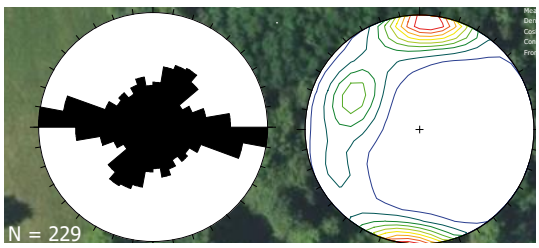

Figure 3: Fracture orientation in the granite of the Saint Pierre Bois quarry

The E-W main set is consistent with the fractures at the regional scale and could be in relation with the tectonic of the Villé basin, which began during Permian and that continues progressively during Triassic, and collapse in Tertiary in relation with the Rhine graben opening (Laubacher & von Eller, 1966).

3.2 Mineral filling of fractures and faults

Numerous of E-W faults provide evidence of striation on dark surfaces, and consist of cohesive fracture/fault cataclasites due to high silicification with minor illite (figure 4). The contacts between fault rocks and wall-rock usually exhibit decreasing brittle deformation.

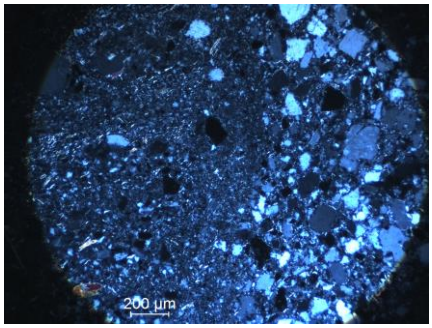

Figure 4: Micrograph of cohesive cataclasis under polarized light in a small fracture showing a fine-grained mixture of micro-quartz and illite with minor feldspars.

The largest faults consist of metric-sized corridors of cohesive cataclasis/breccia showing successive stages of cementation including hematite, barite and quartz. Most of the small structures are plugged by quartz, whereas the largest structures currently show residual porosity on the both sides of the plugged central zone cemented barite and quartz (figures 5 and 6).

Figure 5: Photographs of the both sides of a same sample of the rim of a cohesive breccia in a major fault showing the porosity of this zone.

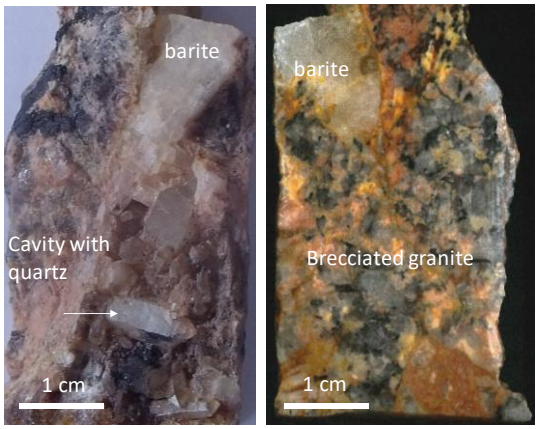

Figure 6: Photographs of the both sides of a small quartz geode and a zone of barite cement.

3.3 Wallrock alteration

Granite matrix associated with E-W faults shows various intensities of alteration. Alteration of the granite matrix is intense close to the cataclasis zone but rapidly decreases at few centimeters far. Far from the faults and fractures, biotite is partially transformed into chlorite, and feldspars are little altered. Close to the fractures and faults, and in the fault corridor, biotite and in less amounts muscovite are transformed into clay minerals with iron hydroxides, primary plagioclase is entirely transformed into clay minerals, whereas K-feldspar shows signs of dissolution. Observations rather show that plagioclase is more altered than K-feldspar. Microfractures crosscut the granite. They are filled with iron hydroxides, quartz, some accessory minerals such as titanium oxides, secondary phosphates. Alumino-phosphate-sulfate (APS) minerals occur as µm-sized grains with clay in replacement of plagioclase, and more rarely in the micro-fractures. The radial morphology of iron hydroxides in residual porosity rather indicates a precipitation in supergene conditions. Most of these iron hydroxides are cemented later by quartz, suggesting that for a part of them, they precipitated during post-Hercynian paleo-weathering, and not during present day weathering.

3.3 Fracture network and porosity

Breccia blocs taken on the rims of a decametric fault corridor (sample of the figure 4) have porosities of 5.5 to 7.5 %. These porosities are higher than porosity of the granite matrix (Kushnir et al., 2018).

Porosity of granite matrix near fractures and cataclasites is low and quite similar to granite reference (2-3 %). Slight variations are due to small feldspar alteration and dissolution.

4. RESERVOIR QUALITY OF STEPHANIAN-PERMIAN SANDSTONES

4.1 Orientation measurements

Sandstones are significantly less fractured than the granitic basement. The two major fracture sets are very similar to those observed in the granitic basement (Figure 7).

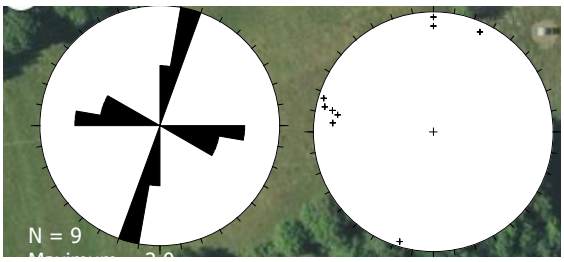

Figure 7: Fracture orientation in the sandstones of the Saint Pierre Bois quarry

4.2 Diagenetic sequence of sandstones

Sandstones are heterogranular medium to coarse-grained arkoses. Detrital minerals consist of quartz, plagioclase and K-feldspar grains, with minor biotite (Bio), muscovite (Mus), tourmaline (Tur), clay matrix, iron hydroxides, and heavy minerals such as zircon, apatite, ilmenite, and monazite. Authigenic minerals are mainly quartz with minor K-feldspar, clay minerals, titanium oxides and aluminium phosphate (APS) minerals. No fracture filling was observed.

Pressure/dissolution features and high degree of recrystallization often obliterate the pristine morphologies of detrital quartz grains. However, the rare preserved detrital quartz grains are generally sub-rounded to rounded based on the dustlines that separate the detrital grain and quartz overgrowths. At least three types of authigenic quartz are identified in all the sandstone samples, based on their texture and relationships with other minerals: 1) early quartz aureoles growing in the continuity of the detrital quartz crystals. Most of these quartz aureoles show present irregular edges suggesting dissolution/recrystallization, 2) xenomorphic quartz filling intergrained spaces and a part of secondary porosity related to feldspar dissolution; this quartz is the major type observed in sandstones, and 3) a micron- to medium grained quartz crystallized or recrystallized at most of the grain contacts with minor clay mineral.

Plagioclase (albite dominant) represents about 10 % of the detrital grains. Most of the plagioclase grains are sericitized (oriented clay particles) or exhibit a high degree of dissolution. Unoriented clay minerals and APS partly filled secondary porosity of dissolution (figure 8).
X-ray diffraction and electron microprobe on separates of authigenic clays rather indicate illite. Microprobe analyses of APS minerals were obtained on few micron-sized crystals in <100 µm-sized aggregates. APS minerals have a calculated average chemical formula:
$(Pb_{0.38}Ce_{0.30}Sr_{0.29}La_{0.16}Ca_{0.09})\ (Al_{0.9}Fe_{0.1})\ (PO_4)_{1.30}\ (SO_4)_{0.15}\ (AsO4)_{0.44}\ (SiO_4)_{0.11}\ (OH)_6$

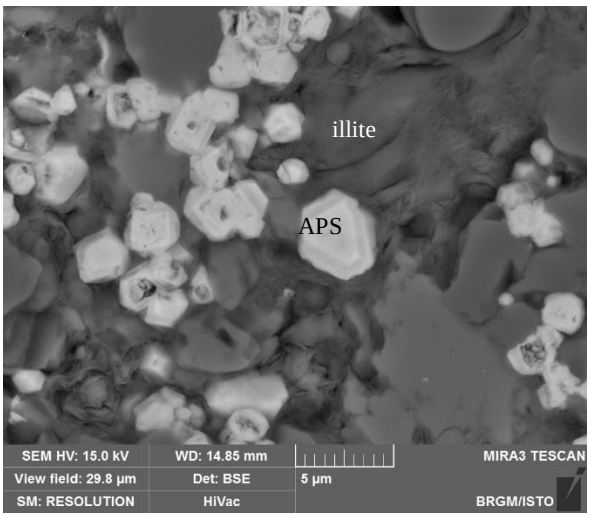

Figure 8: Backscattered electron image showing APS and illite partially filling the porosity of plagioclase dissolution

K-feldspar represents about 15-20 % of the detrital grains. Detrital K-feldspar grains have various morphologies from rounded to almost euhedral grains, suggesting that the source of detrital K-feldspar was not far from the sedimentation site. K-feldspar is more abundant than plagioclase. Its degree of alteration/ dissolution is also lower than those of plagioclase, and even small euhedral authigenic K-feldspar grew on detrital grains. On the other hand both authigenic and detrital K-feldspar grains provide evidence of dissolution signs, indicating that the dissolution process is later than the authigenic K-feldspar cementation.

Among accessory minerals, zircon, monazite and titanium oxides are detrital minerals, which are quite well preserved, whereas ilmenite exhibit high dissolution degree with in-situ reprecipitation of secondary titanium oxides. Galena and pyrite are present in traces. It is noteworthy that titanium oxides are enriched in Nb, Ta and W (figure 9).

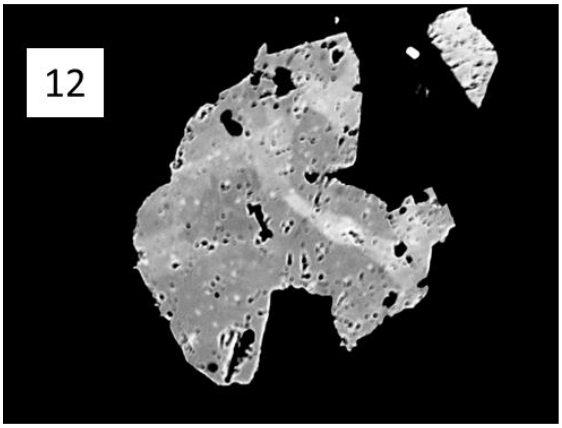

TiO2	Sc	Fe	Cr	Nb	Sn	Ta	W
wt %	mg.kg^{-1}						
97.26		4607		1953		433	7740

Figure 9: Backscattered electron image of a detrital titanium oxide grain showing chemical zoning, and trace element contents measured by electron microprobe.

4.3 Sandstone porosity

Sandstone porosity and porosity of dissolution of the both types of feldspars were measured on ten samples by treatment of backscattered electron images, using the image J software. For total porosity, the measurements were carried out on ten images with a low magnification (figure 10). For feldspars, we measured porosity on more than 20 grains on images with a higher magnification (figure 11).

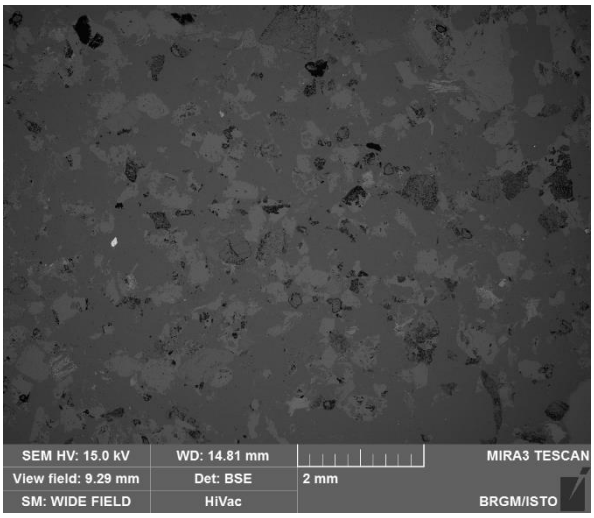

Figure 10: Backscattered electron image used for total porosity measurement

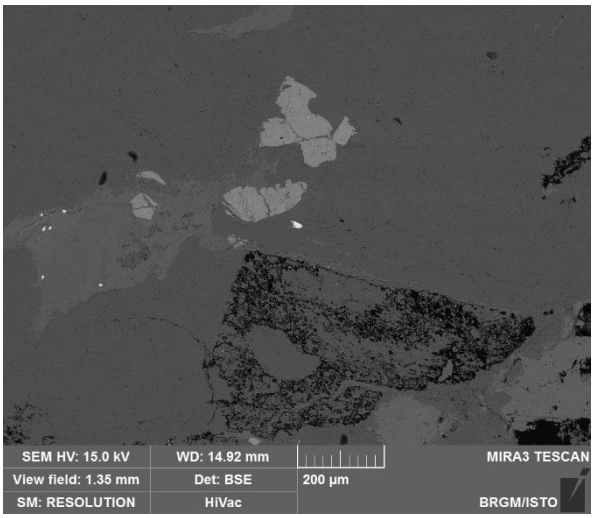

Figure 11: Backscattered electron image used for porosity measurement of feldspar dissolution.

Total porosities measured by image treatment (Φ) are quite consistent with previous data (Kushnir et al., 2018), indicating a large range of porosity between ~5 and 14 % (Table 1).

Complementary porosities of feldspar dissolution provide evidence of a good correlation between total porosity and porosity of plagioclase and K feldspar dissolution (table 1; figure 12). In all cases, porosity of plagioclase dissolution is significantly higher than porosity of K feldspar dissolution (table 1; figure 12).

	Φ	Φ *	Φ Pl	Φ Kfs
SPB1	6.6 ± 1.7	9.3	30.1 ± 3.9	11.1 ± 7.3
SPB2	8.7 ± 0.6	10.1	45.4 ± 12.0	17.4 ± 5.6
SPB3	12.0 ± 1.2	12.4	42.7 ± 12.5	21.4 ± 18.3
SPB5	4.7 ± 1.2	6.4	33.4 ± 17.5	5.5 ± 1.8
SPB6	11.8 ± 2.1	13.4	44.8 ± 20.2	19.4 ± 8.8
SPB7	13.9 ± 1.4	13.0	32.3 ± 5.7	17.1 ± 6.9
SPB8	11.2 ± 1.5	13.5	46.1 ± 12.4	17.8 ± 13.5
SPB10	5.0 ± 1.6	6.3	25.1 ± 5.8	7.1 ± 4.8
SPB11	6.3 ± 1.0	nd	32.2 ± 10.0	8.1 ± 4.3
SPB12	7.1 ± 1.5	10.6	37.5 ± 5.6	15.5 ± 6.6

Table 1: Total porosity measured by image treatment (Φ) compared with total porosity data given in Kushnir et al. (2018), and porosity of plagioclase (Φ Pl) and K-feldspar (Φ Kfs) dissolution measured by image treatment.

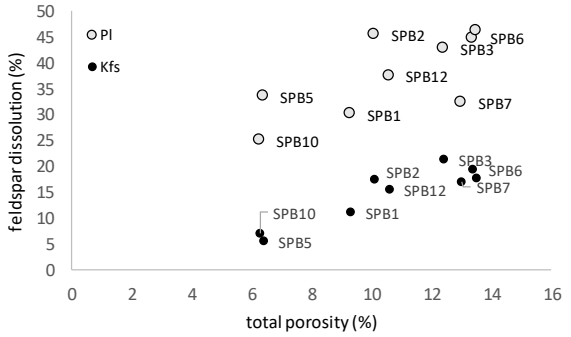

Figure 12: Porosity of feldspar dissolution in function of total porosity (Pl for plagioclase and Kfs for K-feldspar).

5. ROLE OF PALEO-WEATHERING AND COVER/BASEMENT INTERFACE

Hercynian paleo-weathering and Permian tectonics highly controlled the topology of granite erosion paleo-surface, the distribution of the detrital sediments in term of mineralogy and texture, and consequently on the evolution of the petrophysical properties of the sedimentary cover itself. Indeed, we contend that the silty clay layers locally present at the cover/basement transition may act as seals to fluid flow.

In the Saint Pierre Bois quarry, we distinguished:

1) the left side and the back front of quarry, in which granite is slightly weathered and hetero-granular coarse-grained products of in-situ granite dismantling filled the negative relief of the granite erosion surface, and

2) the right side of the quarry, in which the profile of paleo-weathering is well developed in the granitic basement, and faults affect significantly the topology of the transition zone (figure 13). A 30-50 cm thick red silty clay layer overlaid weathered granite.

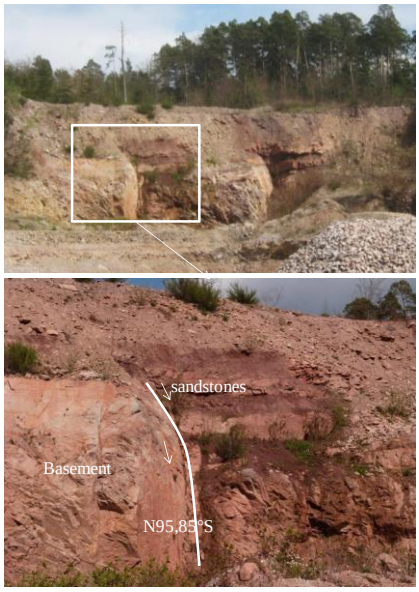

Figure 13: Topology of the transition zone in the right side of quarry marked by fault displacements.

The slightly weathered granite at transition in the back front of the quarry indicates a highly eroded paleo-surface, on contrary to the left side of the quarry.

6. CONCLUSION

The multi-discipinary study of the cover/basement transition in the Saint Pierre Bois quarry provides evidence of two fracture sets (E-W and NNE-SSW) highly developed in the Hercynian granite, and slightly developed in sandstones. The Hercynian fractures of the crystalline basement appear to have been reactivated during the Tertiary, but few new fractures were created through the cover/basement interface to the sedimentary cover. Frequent vertical displacements of blocks are probably of great interest; striated dark reddish planes consist of cohesive fracture/fault rocks (breccia and cataclasite) due to high silicification with minor illite. These cohesive fault rocks are thought to develop at depth in the dominant brittle fracturing zone, and might be informative of deep circulations of hot fluids in the Rhine graben. The presence of authigenic illite and APS in both sandstones and granite confirm it. Detailed study of large cataclastic corridors provides evidence of successive pulses of fluids, rims of the corridors being the most favourable for fluid pathway.

The research leading to these results has received funding from the ANR Programme under grant agreement ANR-15-CE06-0014 (Project CANTARE-Alsace) and from the French Scientific Interest Group for carbon-free energy Géodénergies (REFLET project).

REFERENCES

Blanalt et al., (1970)

Kushnir, A., Heap M.J., Baud P., Gilg H. et al. (2018). Characterizing the physical properties of rocks from the Paleozoic to Permo-Triassic transition in the Upper Rhine Graben. Geothermal Energy vol. 6.